Generalized Approach to Resolution Analysis in BSAR

TAO ZENG
Beijing Institute of Technology

MIKHAIL CHERNIAKOV
University of Birmingham
UK

TENG LONG
Beijing Institute of Technology

Bistatic synthetic aperture radars (BSARs) have been the focus of increasing research activity over the last decade. The generalized ambiguity function (GAF) of bistatic SAR is introduced here. First, the GAF for BSAR is represented in the delay-Doppler domain, and is then expanded to the spatial (coordinates) domain. From the GAF, comprehensive knowledge regarding the resolution of BSAR can be extracted, including the range and azimuth resolutions, as well as the area of a resolution cell of BSAR. These general results are also applied to the performance analysis of several particular BSAR geometries, including the space-surface-BSAR (SS-BSAR) system, to demonstrate the potential ability of this newly introduced system.

Manuscript received October 20, 2003; revised August 24, 2004; released for publication December 27, 2004.

IEEE Log No. T-AES/41/2/849013.

Refereeing of this contribution was handled by P. Lombardo.

Part of this work was supported by EPSRC (UK) under Grant GR/S69221/01.

Authors' addresses: T. Zeng and T. Long, Dept. of Electrical Engineering, Beijing Institute of Technology, Dept. EE 551 Lab, No. 5 Zhongg uancun, Nandajie, PO Box 327, Beijing 10081, China, E-mail: (zengtao@bit.edu.cn); M. Cherniakov, University of Birmingham, Communications Engineering Group, Edgbaston, Birmingham, B15 2TT, UK.

NOMENCLATURE

f_c	Carrier frequency
$h_{\mathbf{A}}(t,u)$	Returned signals
$m_A(f_d)$	Inverse Fourier transform of $\bar{M}_A(u)$
$p(\tau_d)$	Inverse Fourier transform of $\bar{P}(f)$
$s(t)$	Complex envelope of transmitted signal
t,u	Fast and slow time
u_A	Slow time instant which maximizes $M_A(u)$
$G'_{\mathrm{T}}(\mathbf{A},u)$, $G'_{\mathrm{R}}(\mathbf{A},u)$	Gain of the antenna
$G_{\mathrm{T}}(.)$, $G_{\mathrm{R}}(.)$	Antennas' radiation pattern
$M_A(u)$	Power ratio between received and transmitted signals
$P(f)$	Power spectrum of ranging signal
$\mathbf{W}_{\mathrm{R}}$, $\mathbf{W}_{\mathrm{T}}$	Position vectors of transmitter and receiver
$\mathbf{V}_{\mathrm{R}}$, $\mathbf{V}_{\mathrm{T}}$	Velocity vectors of transmitter and receiver
τ_d	Differential delay
$\tau_A(u)$	Time delay of received signal at slow time u
f_d	Differential Doppler frequency
$\bar{P}(f)$	Normalized ranging signal power spectrum
$\bar{M}_A(u)$	Normalized received signal magnitude pattern
α	Angle between $\mathbf{\Theta}$ and $\mathbf{\Xi}$
β	Bistatic angle
δ_τ	Delay resolution
δ_D	Doppler resolution
δ_r	Range resolution
δ_a	Azimuth resolution
δ_c	Cross range resolution
$\delta_{\mathbf{\Omega}}$	Resolution in direction of $\mathbf{\Omega}$
δ_f	-3 dB widths of $\bar{P}(f)$
δ_u	-3 dB widths of $\bar{M}_A(u)$
θ_τ	Angle between $\mathbf{\Omega}$ and $\mathbf{\Theta}$
θ_a	Angle between $\mathbf{\Omega}$ and $\mathbf{\Xi}$
ω_{TA}, ω_{RA}	Angular speeds of transmitter and receiver
ω_{E}	Equivalent angular speed
$\mathbf{\Gamma}_{\mathrm{T}}$, $\mathbf{\Gamma}_{\mathrm{R}}$	Directions of effective velocities
$\mathbf{H}$	Unit vector which is perpendicular to both vectors $\mathbf{\Theta}$ and $\mathbf{N_b}$
$\mathbf{\Theta}$	Direction of bisector of bistatic angle
$\mathbf{N_b}$	Unit vector in direction of normal line to basic plane
$\mathbf{\Xi}$	Direction of equivalent motion
$\mathbf{\Phi}_{\mathbf{TA}}$, $\mathbf{\Phi}_{\mathbf{RA}}$	Unit vector in direction of line of sight.

I. INTRODUCTION

Bistatic synthetic aperture radars (BSARs) have been the focus of increasing research activity over the last decade. This reflects the progress in synthetic aperture radar (SAR) technology, both hardware and software, satellite positioning systems that allow synchronising BSAR subsystems, as well as achievements in aerospace technology. The engine behind this is a strong demand for the further improvement in the performance of microwave remote sensing systems, and it is expected that the practical utilisation of BSARs will respond to this demand [1]. BSAR can be used to obtain essentially new information regarding land and ocean surfaces [2], operate as the remote change detectors to predict natural disasters [3], effectively use noncooperative transmitters that reduce system costs [4], or similarly act as an auxiliary subsystem to existing monostatic SARs [5].

One of the key parameters of any remote sensing system is the spatial resolution. In traditional radar systems, comprehensive knowledge regarding the resolution can be obtained from the ambiguity function (AF) analysis [6], in terms of delay (range) and Doppler frequency (speed). Definition of a generalized AF (GAF) was expanded in spatial resolution in SAR [7]. Similarly, in the SAR system analysis the point spread function (PSF) is used to characterize spatial resolution [8]. The GAF is used here for BSAR analysis to unify the approach between traditional aperture radars and SARs.

The basic information regarding bistatic radar can be found in classic texts [9]. If the transmitter and the receiver are stationary or following parallel trajectories during the coherent integration time, they can be considered as a space (time)-invariant system. Meanwhile, there are a number of new forthcoming researches in BSAR [1, 4, 10, 11], along with others, in which the transmitter and the receiver have their own nonparallel trajectories. From the point of view of system analysis, this means that BSAR are no longer space (time)-invariant systems. Their resolution essentially depends on the observation time instant and space-variant analysis should be considered in evaluating BSAR spatial resolution.

In [9], the resolution issue of BSAR is studied in two-dimensional space, which is a relatively simple case of BSAR geometry. In [12], several of the resolution equations have been researched via the use of gradient analysis. These equations can cover the general BSAR geometry, but only apply to the rectangular spectrum shape of the ranging signal. In order to achieve a comprehensive insight into the problem of spatial resolution analysis, a more generalized approach is needed. The resolution analysis is carried out here via an introduction of BSAR spatial GAFs. This general approach is applicable for BSAR with essentially different configurations and can obtain the resolution in an arbitrary direction. The AF for the ground-based bistatic radar has been brought forward in [21]. Because of the significant difference between the geometry of the groundbased bistatic radar and that of BSAR, the AF introduced in [21] is quite different from the AF in this work. For example, the former is established on the delay-velocity plane, while the latter is on the x-y-z coordinate system. Besides the resolution in a given line, the area of the resolution cell can also be found via the AF. The resolution cell area is a good parameter to show the resolvability of a system, but up until now only a few papers have discussed this issue. One such paper is [22]. Unfortunately, the results of [22] are not applicable to BSAR, because the resolution cell area depends directly on the widths of the antenna lobes of the radar system.

In this paper, the GAF for BSAR is first represented in the delay-Doppler domain, and then expanded to the spatial (coordinates) domain. Using this spatial presentation of GAF the range and azimuth resolution, as well as a resolution cell area are considered relevant to different directions and coordinate systems. Finally, obtained equations are applied to the resolution analysis in space-surface BSAR (SS-BSAR).

II. AMBIGUITY FUNCTION OF BSAR

A. BSAR System Geometry

The generalized topology of BSAR is shown in Fig. 1. Vectors $\mathbf{W}_R$, $\mathbf{W}_T$ are the position vectors of the transmitter and receiver respectively in the rectangular coordinate xyz; $\mathbf{V}_R$, $\mathbf{V}_T$ are their velocity vectors (they are assumed constant here), $\mathbf{A}$ is a vector which specifies an arbitrary position in the target area, and $\mathbf{W}_T - \mathbf{A}$ (or $\mathbf{W}_R - \mathbf{A}$) are called the transmitter (or receiver) line of sight.

As the first step in evaluating the radar's resolution, we describe a received signal model in BSAR. Despite the fact that the transmitter and the receiver possess a continuous motion, in practical situations the stop-and-go approach [8] can be used for SAR analysis, namely, during the ranging signal propagation along the transmitter-target-receiver path, the transmitter and receiver are assumed to be stationary, a radar measurement is made, and then they move to the next spatial positions. According to this assumption, the received signal is modeled as a function of two variables. One variable is the fast time t, which describes the ranging waveform and its propagation. The second variable u is the slow time, which specifies the position of the transmitter and the receiver. The term "slow time" comes from the fact that the motions of the transmitter and receiver are

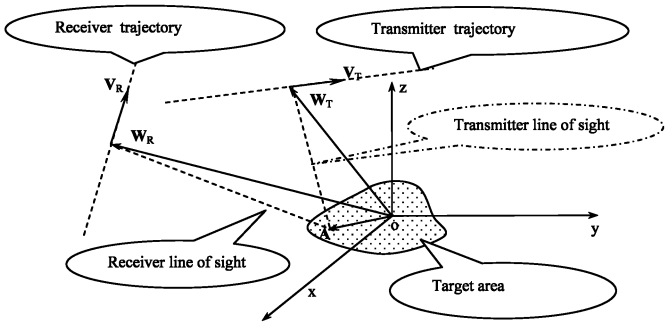

Fig. 1. Generalized topology of BSAR.

much slower than the speed of the electromagnetic wave propagation. Thus in slow time instant u, the positions of the transmitter and receiver are

$$\begin{aligned}\mathbf{W}_{\mathrm{T}}(u) &= \mathbf{W}_{\mathrm{T}}(0) + u\mathbf{V}_{\mathrm{T}} \\ \mathbf{W}_{\mathrm{R}}(u) &= \mathbf{W}_{\mathrm{R}}(0) + u\mathbf{V}_{\mathrm{R}}\end{aligned} \tag{1}$$

where $\mathbf{W}_{\mathrm{R}}(0)$ and $\mathbf{W}_{\mathrm{T}}(0)$ are the positions of the transmitter and receiver at the slow time instant $u = 0$.

Let the transmitted signal be $s(t)\exp(j2\pi f_c t)$, where f_c is the carrier frequency, $s(t)$ is the complex envelope of the transmitted signal. If a point target with unit radar cross section (RCS) is at position $\mathbf{A}$, the corresponding received signal at the output of the receiver antenna can be represented as

$$h_{\mathbf{A}}(t,u) = \sqrt{M_A(u)}s[t-\tau_A(u)]\exp[j2\pi f_c(t-\tau_A(u))]. \tag{2}$$

In this equation, $\tau_A(u)$ is the time delay of the received signal at slow time u

$$\tau_A(u) = \frac{|\mathbf{A}-\mathbf{W}_{\mathrm{T}}(u)| + |\mathbf{A}-\mathbf{W}_{\mathrm{R}}(u)|}{c} \tag{3}$$

$M_A(u)$ is the power ratio between the received and the transmitted signals:

$$M_{\mathbf{A}}(u) = \frac{1}{(4\pi)^3}\frac{\lambda^2 G'_{\mathrm{T}}(\mathbf{A},u)}{|\mathbf{A}-\mathbf{W}_{\mathrm{T}}(u)|^2}\frac{G'_{\mathrm{R}}(\mathbf{A},u)}{|\mathbf{A}-\mathbf{W}_{\mathrm{R}}(u)|^2} \tag{4}$$

where c is the speed of the light, λ is the wavelength, $G'_{\mathrm{T}}(\mathbf{A},u)$ and $G'_{\mathrm{R}}(\mathbf{A},u)$ are the gain of the transmitter and the receiver antennas at slow time instant u in the direction of the target.

B. Derivation of Ambiguity Function for BSAR

In most cases, a signal at the output of the receiver antenna is a superimposition of a large number of reflections from different objects within an illuminating area. One of the main parameters that characterizes SAR performance is its spatial resolution, i.e., the minimum distance between two targets that can be separately received at the output of a matched filter. The most comprehensive information regarding the radar resolution can be obtained from the GAF [7]. According to [7] and using notations specified in this paper, the GAF is defined as

$$\begin{aligned}\chi(\mathbf{A},\mathbf{B}) &= \frac{\iint h_{\mathbf{A}}(t,u)h^*_{\mathbf{B}}(t,u)dt\,du}{\sqrt{\iint |h_{\mathbf{A}}(t,u)|^2 dt\,du}\sqrt{\iint |h_B(t,u)|^2 dt\,du}} \\ &= \frac{\begin{array}{r}\iint \sqrt{M_A(u)}\sqrt{M_B(u)}s[t-\tau_A(u)]s^*[t-\tau_B(u)] \\ \times\exp[j2\pi f_c(\tau_B(u)-\tau_A(u))]dt\,du\end{array}}{\begin{array}{r}\sqrt{\iint M_A(u)|s[t-\tau_A(u)]|^2 dt\,du} \\ \times\sqrt{\iint M_B(u)|s[t-\tau_B(u)]|^2 dt\,du}\end{array}}.\end{aligned} \tag{5}$$

In this equation, vector $\mathbf{A}$ indicates the position of the desired point reflection to be evaluated, vector $\mathbf{B}$ is an arbitrary position of another reflector in a vicinity of $\mathbf{A}$. $h_{\mathbf{A}}(t,u)$ and $h_{\mathbf{B}}(t,u)$ are the signals returned from these reflectors. Equation (5) shows that the AF is introduced as the correlation coefficient between waveforms reflected from two spatially separated targets, i.e., $h_{\mathbf{A}}(t,u)$ and $h_{\mathbf{B}}(t,u)$. This has a physical explanation: the level of the spatial discrimination of two point targets depends on the difference of these two waveforms reflected from the targets and the difference of the functions is mathematically characterized by their correlation coefficient.

When (5) introduces the ambiguity presented in time domain, for future analysis it is convenient to present this function in frequency domain. Using Parseval's theorem and (2)–(4) we obtained

$$\begin{aligned}&\chi(\mathbf{A},\mathbf{B}) = \\ &\frac{\begin{array}{r}\int\Big\{P(f)\exp[j2\pi f[\tau_B(u)-\tau_A(u)]]\int\sqrt{M_A(u)M_B(u)} \\ \times\exp[j2\pi f_c[\tau_B(u)-\tau_A(u)]]du\Big\}df\end{array}}{\sqrt{\iint P(f)M_A(u)df\,du}\sqrt{\iint P(f)M_B(u)df\,du}}\end{aligned} \tag{6}$$

where $P(f)$ is the power spectrum of the ranging signal. That is the BSAR GAF presented signals in the frequency domain.

In order to simplify the equation for the AF, several practically applicable assumptions can be stated as follows.

1) Power of signals reflected from targets A and B are approximately equal: $M_B(u) \approx M_A(u)$. This assumption follows on from the definition of the GAF: the targets have unit RCS and the correlation analysis is specified in a vicinity of $\mathbf{A}$, consequently we can assumes the targets are illuminated by the same antenna patterns.

2) The synthetic aperture is narrow. Denoting the slow time instant which maximizes $M_A(u)$ as u_A and the -3 dB width of $M_A(u)$ as δ_u, i.e., $M\left(u_A - (\delta_u/2)\right) = (\frac{1}{2})M(u_A)$. The synthetic aperture is narrow means that $V_{\mathrm{T}}\delta_u \ll W_{\mathrm{T}}(u_A)$ and $V_{\mathrm{R}}\delta_u \ll W_{\mathrm{R}}(u_A)$, i.e., the lengths of the synthetic apertures are much smaller than the lengths of the line of sight at the slow time instant u_A. Due to this assumption, the phase term of the inner folder integral in (6) can be approximated by its first-order Taylor expansion at $u = u_A$

$$2\pi f_c[\tau_B(u) - \tau_A(u)] \approx 2\pi f_c \tau_d + 2\pi f_d(u - u_A). \quad (7)$$

In this equation, τ_d is the delay difference between the two signals when $u = u_A$

$$\tau_d = \frac{|\mathbf{B} - \mathbf{W}_{\mathrm{T}}(u_A)| + |\mathbf{B} - \mathbf{W}_{\mathrm{R}}(u_A)|}{c} - \frac{|\mathbf{A} - \mathbf{W}_{\mathrm{T}}(u_A)| + |\mathbf{A} - \mathbf{W}_{\mathrm{R}}(u_A)|}{c} \quad (8)$$

and f_d is the difference of the Doppler frequency between these two signals at u_A

$$f_d = \frac{f_c}{c}\left[\mathbf{V}_{\mathrm{T}}^{\mathrm{T}}\frac{\mathbf{B} - \mathbf{W}_{\mathrm{T}}(u_A)}{|\mathbf{B} - \mathbf{W}_{\mathrm{T}}(u_A)|} + \mathbf{V}_{\mathrm{R}}^{\mathrm{T}}\frac{\mathbf{B} - \mathbf{W}_{\mathrm{R}}(u_A)}{|\mathbf{B} - \mathbf{W}_{\mathrm{R}}(u_A)|}\right] - \frac{f_c}{c}\left[\mathbf{V}_{\mathrm{T}}^{\mathrm{T}}\frac{\mathbf{A} - \mathbf{W}_{\mathrm{T}}(u_A)}{|\mathbf{A} - \mathbf{W}_{\mathrm{T}}(u_A)|} + \mathbf{V}_{\mathrm{R}}^{\mathrm{T}}\frac{\mathbf{A} - \mathbf{W}_{\mathrm{R}}(u_A)}{|\mathbf{A} - \mathbf{W}_{\mathrm{R}}(u_A)|}\right]. \quad (9)$$

3) The ranging signal is narrowband. Denoting the -3 dB width of $P(f)$ as δ_f, then δ_f should be small enough so that the phase term of the outer folder integral in (6) can be approximated by the phase at slow time u_A:

$$2\pi f[\tau_B(u) - \tau_A(u)] \approx 2\pi f \tau_d. \quad (10)$$

In order to guarantee (10) to be a good approximation, the -3 dB bandwidth ranging signal δ_f must satisfy the condition:

$$\delta_f < \frac{1}{2|[\tau_B(u) - \tau_A(u)] - \tau_d|}$$

$$\text{for all } u \text{ in the interval } |u - u_A| < \tfrac{1}{2}\delta_u. \quad (11)$$

The time resolution is the reciprocal signal bandwidth, hence the physical meaning of (11) is that in the slow time interval $|u - u_A| < \frac{1}{2}\delta_u$, the change of the delay difference should not exceed half of the time resolution cell.

Due to these approximations, (6) can be reduced as

$$\chi(\mathbf{A},\mathbf{B}) = \exp(j2\pi f_c\tau_d)\int_{-\infty}^{\infty}\bar{P}(f)\exp(j2\pi f\tau_d)df \times \int_{-\infty}^{\infty}\bar{M}_A(u)\exp(j2\pi f_d u)du = \exp(j2\pi f_c\tau_d)p(\tau_d)m_A(f_d) \quad (12)$$

where $\bar{P}(f) = (P(f)/\int_{-\infty}^{\infty}P(f)df)$ and $\bar{M}_A(u) = (M_A(u + u_A)/\int_{-\infty}^{\infty}M_A(u + u_A)du)$ are the normalized ranging signal power spectrum and the normalized received signal magnitude pattern, $p(\tau_d)$ is the inverse Fourier transform (IFT) of $\bar{P}(f)$, and $m_A(f_d)$ the IFT of $\bar{M}_A(u)$.

Equation (12) indicates that the amplitude of the AF is presented as the product of two functions. The first one is the IFT of the signal power spectrum, hence it is the autocorrelation function of the ranging signal and specifies the SAR delay resolution. The second term $m_A(f_d)$ is the IFT of the normalized received signal magnitude pattern and responsible for the Doppler resolution. For a particular BSAR, $\bar{P}(f)$ and $\bar{M}_A(u)$ are known, and the AF can be found by applying the IFT to these functions. In many practical cases these transforms can be obtained from Fourier transform tables [14] and consequently the -3 dB widths of the system's delay (δ_τ) and Doppler (δ_D) resolution cells can be calculated by

$$\delta_\tau = 2p^{-1}\left[\frac{p(0)}{\sqrt{2}}\right], \qquad \delta_D = 2m_A^{-1}\left[\frac{m_A(0)}{\sqrt{2}}\right] \quad (13)$$

where $p^{-1}(.)$ and $m_A^{-1}(.)$ are the inverse functions of $p(.)$ and $m_A(.)$.

For the sake of solidity, but without loss of generality, we consider two typical cases, namely, when antenna patterns and ranging waveform can be approximated by a Gaussian or rectangle shape functions. IFTs of these functions are shown in Table I, where

$$\mathrm{sinc}(x) = \frac{\sin x}{x}. \quad (14)$$

In the case of the Gaussian model, the resolutions can be found directly from (13):

$$\delta_\tau = \frac{2\ln 2}{\pi\delta_f}, \qquad \delta_D = \frac{2\ln 2}{\pi\delta_u} \quad (15)$$

where δ_f and δ_u are the -3 dB widths of $\bar{P}(f)$ and $\bar{M}_A(u)$.

In the rectangular model, the inverse function cannot be expressed in closed form, but according to the scaling property of the Fourier transform

TABLE I
IFTs of Gaussian Function and Rectangle Pulse Function

Model Type	Function	IFT
Gaussian model	$\frac{1}{\sqrt{2\pi}a}\exp\left(-\frac{y^2}{2a^2}\right)$	$\exp(-2\pi^2a^2x^2)$
Rectangular shape model	$\begin{cases}\frac{1}{a} & -\frac{a}{2}<y<\frac{a}{2}\\ 0 & \text{otherwise}\end{cases}$	$\text{sinc}(\pi ax)$

[14], the widths of the resolution cells are inversely proportional to the widths of their counterparts of $\bar{P}(f)$ and $\bar{M}_A(u)$ and the proportional coefficient has been found numerically:

$$\begin{aligned}\delta_\tau &= 0.886/\delta_f\\ \delta_D &= 0.886/\delta_u.\end{aligned} \tag{16}$$

Thus far, we have obtained the representation of AF of BSAR in quite a general form, and we have also found the values of the delay and Doppler resolutions. In order to have an insight into the AF, we now perform a further analysis on $\bar{M}_A(u)$. In most practical scenarios of the BSAR systems, the impact of change of the slant distance in the slow time interval $|u-u_A|<\frac{1}{2}\delta_u$ can be ignored, and as a result, $\bar{M}_A(u)$ is approximately determined by the combined antenna beam:

$$\bar{M}_{\mathbf{A}}(u)=\frac{G'_{\mathrm{T}}(\mathbf{A},u)G'_{\mathrm{R}}(\mathbf{A},u)}{\int G'_{\mathrm{T}}(\mathbf{A},u)G'_{\mathrm{R}}(\mathbf{A},u)du}. \tag{17}$$

Generally speaking, the form of the combined beam is specified by a set of quite complex factors, e.g. the transmitter and the receiver trajectories, the scan patterns of the antennas, and the gains of the antennas. But if the receiver and the transmitter are moving in parallel and the directions of the antennas are fixed with respect to the trajectories, $\bar{M}_A(u)$ has a relatively simple form:

$$\bar{M}_A(u)=\frac{\begin{array}{c}G_{\mathrm{T}}[\theta_{\mathrm{T}A}+\omega_{\mathrm{T}A}\times(u-u_A)]\\ \times G_{\mathrm{R}}[\theta_{\mathrm{R}A}+\omega_{\mathrm{R}A}\times(u-u_A)]\end{array}}{\begin{array}{c}\int_{-\infty}^{\infty}G_{\mathrm{T}}[\theta_{\mathrm{T}A}+\omega_{\mathrm{T}A}\times(u-u_A)]\\ \times G_{\mathrm{R}}[\theta_{\mathrm{R}A}+\omega_{\mathrm{R}A}\times(u-u_A)]du\end{array}}. \tag{18}$$

In this equation, $G_{\mathrm{T}}(.)$ and $G_{\mathrm{R}}(.)$ are the appropriate antennas' radiation patterns; $\theta_{\mathrm{T}A}$ is the angle between the transmitter antenna's electronic axis and the transmitter line of sight at slow time instant u_A; $\theta_{\mathrm{R}A}$ has the similar meaning; $\omega_{\mathrm{T}A}$, $\omega_{\mathrm{R}A}$ are the angular speeds of the transmitter and the receiver with respect to $\mathbf{A}$ at slow time instant u_A. These angular speeds can be introduced in vector notations:

$$\begin{aligned}\omega_{\mathrm{T}A}&=\frac{|[\mathbf{I}-\mathbf{\Phi}_{\mathrm{T}\mathbf{A}}\mathbf{\Phi}_{\mathrm{T}A}^{\mathrm{T}}]\mathbf{V}_{\mathrm{T}}|}{|\mathbf{W}_{\mathrm{T}}(u_A)-\mathbf{A}|}\\ \omega_{\mathrm{R}A}&=\frac{|[\mathbf{I}-\mathbf{\Phi}_{\mathrm{R}\mathbf{A}}\mathbf{\Phi}_{\mathrm{R}A}^{\mathrm{T}}]\mathbf{V}_{\mathrm{R}}|}{|\mathbf{W}_{\mathrm{R}}(u_A)-\mathbf{A}|}\end{aligned} \tag{19}$$

where $\mathbf{I}$ is the 3×3 unit matrix, $\mathbf{\Phi}_{\mathrm{T}\mathbf{A}}$ (or $\mathbf{\Phi}_{\mathrm{R}\mathbf{A}}$) is the unit vector in the direction of the transmitter's (or receiver's) line of sight for $\mathbf{A}$ at slow time u_A.

The above equations state that the term of $\bar{M}_A(u)$ covers the properties of antenna radiation patterns and the system's geometry. This highlights the difference between the GAF and the well-known Woodward AF [6]. The Woodward AF is fully specified by the waveform of the ranging signal. In contrast, the information carried by the GAF includes not only the ranging signal waveform, but also the antennas and the trajectories. The other difference between the GAF and the Woodward AF is that the Woodward AF is defined on the delay-Doppler plane, but the GAF is fundamentally a function of the spatial coordinates. This point is discussed in detail in the next section.

III. SPATIAL RESOLUTION OF BSAR

A. Resolution Directions

Fundamentally, (12) introduces the BSAR AF and consequently fully characterizes its resolution in terms of the time delay τ_d and the Doppler frequency f_d. Nevertheless, taking into account an essentially space-variant nature of BSAR and the fact that these variables are derived directly from the transmitter-target-receiver coordinates and their dynamics, it is important to expresses the AF directly as the function of the coordinates vectors and obtain the spatial resolution of BSAR.

Using Taylor's expansion of τ_d with respect to $\mathbf{B}$ at the point $\mathbf{B}=\mathbf{A}$, (8) becomes

$$\tau_d\approx\frac{[\mathbf{\Phi}_{\mathrm{T}A}+\mathbf{\Phi}_{\mathrm{R}A}]^{\mathrm{T}}(\mathbf{B}-\mathbf{A})}{c} \tag{20}$$

where $\mathbf{\Phi}_{\mathrm{T}A}$ and $\mathbf{\Phi}_{\mathrm{R}A}$ are the unit vectors in the direction of the transmitter's and receiver's line of sight. Similarly f_d (9) obtains the form:

$$f_{\mathrm{d}}\approx\frac{1}{\lambda}[\omega_{\mathrm{T}A}\mathbf{\Gamma}_{\mathrm{T}}+\omega_{\mathrm{R}A}\mathbf{\Gamma}_{\mathrm{R}}]^{\mathrm{T}}(\mathbf{B}-\mathbf{A}) \tag{21}$$

where $\mathbf{\Gamma}_{\mathrm{T}}$ is the unit vector in the direction of the transmitter's effective motion, i.e., perpendicular component of $\mathbf{V}_{\mathrm{T}}$ regarding to $\mathbf{\Phi}_{\mathrm{T}A}$. $\mathbf{\Gamma}_{\mathrm{R}}$ is defined in the same way, hence:

$$\begin{aligned}\mathbf{\Gamma}_{\mathrm{T}}&=\frac{[\mathbf{I}-\mathbf{\Phi}_{\mathrm{T}A}\mathbf{\Phi}_{\mathrm{T}A}^{\mathrm{T}}]\mathbf{V}_{\mathrm{T}}}{|[\mathbf{I}-\mathbf{\Phi}_{\mathrm{T}A}\mathbf{\Phi}_{\mathrm{T}A}^{\mathrm{T}}]\mathbf{V}_{\mathrm{T}}|}\\ \mathbf{\Gamma}_{\mathrm{R}}&=\frac{[\mathbf{I}-\mathbf{\Phi}_{\mathrm{R}A}\mathbf{\Phi}_{\mathrm{R}A}^{\mathrm{T}}]\mathbf{V}_{\mathrm{R}}}{|[\mathbf{I}-\mathbf{\Phi}_{\mathrm{R}A}\mathbf{\Phi}_{\mathrm{R}A}^{\mathrm{T}}]\mathbf{V}_{\mathrm{R}}|}.\end{aligned} \tag{22}$$

Substituting (20) and (21) into (12), the AF becomes

$$\chi(\mathbf{A},\mathbf{B}) \approx \exp\left(j2\pi\frac{[\mathbf{\Phi}_{TA}+\mathbf{\Phi}_{RA}]^{T}(\mathbf{B}-\mathbf{A})}{\lambda}\right) p \times \left(\frac{[\mathbf{\Phi}_{TA}+\mathbf{\Phi}_{RA}]^{T}(\mathbf{B}-\mathbf{A})}{c}\right) m_A \times \left(\frac{[\omega_{TA}\mathbf{\Gamma}_{T}+\omega_{RA}\mathbf{\Gamma}_{R}]^{T}(\mathbf{B}-\mathbf{A})}{\lambda}\right). \quad (23)$$

In order to uncover the physical meaning of (23), several new notations are introduced and the alternative form of the AF is deduced as

$$\chi(\mathbf{A},\mathbf{B}) \approx \exp\left(j2\pi\frac{[\mathbf{\Phi}_{TA}+\mathbf{\Phi}_{RA}]^{T}(\mathbf{B}-\mathbf{A})}{\lambda}\right) p \times \left(\frac{2\cos(\beta/2)\mathbf{\Theta}^{T}(\mathbf{B}-\mathbf{A})}{c}\right) m_A \times \left(\frac{2\omega_{E}\mathbf{\Xi}^{T}(\mathbf{B}-\mathbf{A})}{\lambda}\right) \quad (24)$$

where β is the bistatic angle (the angle between $\mathbf{\Phi}_{TA}$ and $\mathbf{\Phi}_{RA}$) and $\mathbf{\Theta}$ is the unit vector in the direction along the bisector of β; ω_{E} and $\mathbf{\Xi}$ are the module and unit vector of $(\omega_{TA}\mathbf{\Gamma}_{T}+\omega_{RA}\mathbf{\Gamma}_{R})/2$, respectively. Equation (24) indicates that the BSAR system specifies two resolution directions. Following the definitions established by the radar community, they are the range resolution and azimuth resolutions. The range resolution is in the direction of $\mathbf{\Theta}$, i.e., the bisector of the bistatic angle. The azimuth resolution is in the direction of $\mathbf{\Xi}$. ω_{E} and $\mathbf{\Xi}$ are referred to as the equivalent angular speed and the equivalent motion direction, respectively, in this paper. The reason for this is that if a monostatic SAR is moving along the direction of $\mathbf{\Xi}$ with angular speed ω_{E}, it will be equivalent to the BSAR in terms of its azimuth resolution characteristics.

It should be mentioned that in the BSAR system, the azimuth resolution direction, in most cases, is not normal to the range resolution direction. This is an important difference between BSAR and the monostatic SAR for the resolution analysis. Another observation should also be kept in mind: the most significant plane in the monostatic SAR system is the slant plane [9] which is the plane determined by the radar trajectory and the view direction. But in BSAR systems, the plane with a similar impact is specified by the vectors $\mathbf{\Theta}$ and $\mathbf{\Xi}$, i.e., the range resolution direction and the azimuth resolution direction. This plane is referred to as the basic plane. The BSAR system is a two-dimensional imaging system and both resolution directions are confined to the basic plane. As a result, the BSAR system has no resolvability in the direction perpendicular to the basic plane. In another words, the BSAR resolution cell is like a pillar standing on the basic plane. Another point that should be stated is that although the phase term of AF has no contribution to the system resolution, it does play a significant role in the interferometric BSAR performance analysis, which is out of the range of the work presented here.

B. Quantitive Presentation of the Resolution

Quantitatively, the spatial resolvability of a BSAR system is characterized by the -3 dB widths of the range and azimuth resolution cells, denoted as δ_r and δ_a. From (12), (15), (16), and (22), the calculating equations for δ_r and δ_a are

$$\delta_r = \frac{\delta_\tau c}{2\cos(\beta/2)} = \begin{cases} \dfrac{2\ln 2c}{2\cos(\beta/2)\pi\delta_f} & \text{Gaussian model} \\ \dfrac{0.886c}{2\cos(\beta/2)\delta_f} & \text{Rectangular model} \end{cases} \quad (25)$$

and

$$\delta_a = \frac{\delta_D\lambda}{2\omega_{E}} = \begin{cases} \dfrac{2\ln 2\lambda}{2\omega_{E}\pi\delta_u} & \text{Gaussian model} \\ \dfrac{0.886\lambda}{2\omega_{E}\delta_u} & \text{Rectangular model} \end{cases}. \quad (26)$$

In several papers, e.g. [9] and [12], the cross range resolution δ_c is defined, this is due to the fact that the azimuth resolution and the range resolution are not necessarily orthogonal in BSAR. Denoting the angle between $\mathbf{\Theta}$ and $\mathbf{\Xi}$ as α, the cross range resolution can be easily calculated via the following equation:

$$\delta_c = \frac{\delta_a}{\sin\alpha}. \quad (27)$$

In many cases, the resolution should be specified relevant to a particular coordinate system. This new coordinate system does not necessarily coincide with the $\mathbf{\Theta}$ and $\mathbf{\Xi}$ directions. We should recall here that BSARs are space-variant systems and $\mathbf{\Theta}$ and $\mathbf{\Xi}$ are varying in space. Therefore the equation, which specifies the BSAR resolution in an arbitrary direction, is needed. Let $\mathbf{\Omega}$ be the unit vector in the arbitrary direction in 3-D space, the -3 dB resolution in the direction of $\mathbf{\Omega}$, i.e., δ_{Ω}, is

$$p\left(\frac{\delta_{\Omega}\cos\theta_\tau\cos\frac{\beta}{2}}{c}\right) m_A\left(\frac{\delta_{\Omega}\cos\theta_a\omega_{E}}{\lambda}\right) = \frac{1}{\sqrt{2}} \quad (28)$$

where θ_τ is the angle between $\mathbf{\Omega}$ and $\mathbf{\Theta}$, and θ_a is the angle between $\mathbf{\Omega}$ and $\mathbf{\Xi}$. For the Gaussian model, the

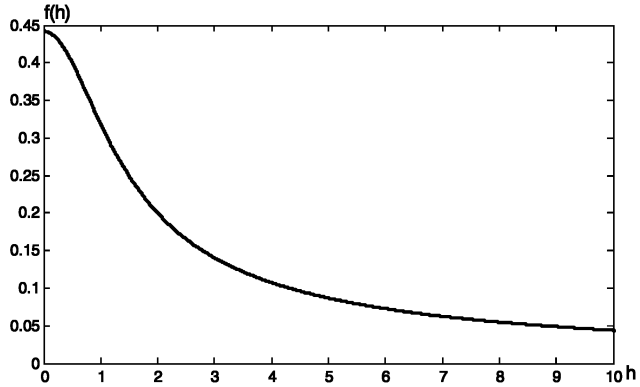

Fig. 2. Dependence of (29) roots on h.

resolution can be obtained directly by solving (28):

$$\delta_{\Omega} = \ln 2 \left[\frac{\pi^2 \delta_f^2 \cos^2\theta_\tau \cos^2\left(\frac{\beta}{2}\right)}{c^2} + \frac{\pi^2 \delta_u^2 \cos^2\theta_a \omega_{\mathrm{E}}^2}{\lambda^2} \right]^{-1/2}$$

$$= \frac{1}{\sqrt{\cos^2\theta_\tau/\delta_r^2 + \cos^2\theta_a/\delta_a^2}}. \tag{29}$$

In the rectangular shape model, (28) is not analytically solvable, so we turn to the numerical method. Changing the variable in (28) from δ_{Ω} to x, where $x = (\delta_{\Omega}\delta_f \cos(\beta/2)\cos\theta_\tau/c)$, it follows:

$$\mathrm{sinc}(\pi x)\mathrm{sinc}(h\pi x) = \frac{1}{\sqrt{2}} \tag{30}$$

with

$$h = \frac{c\delta_u \omega_{\mathrm{E}} \cos\theta_a}{\lambda \delta_f \cos(\beta/2)\cos\theta_\tau}. \tag{31}$$

Referring to the positive root of (30) as $f(h)$, it can be found by the numerical method, and the result is shown in Fig. 2. For the particular system, δ_r, δ_a, θ_τ and θ_a are known, so h can be calculated by (29) and the value of $f(h)$ be found from Fig. 2. The final expression of the resolution is

$$\delta_{\Omega} = \frac{cf(h)}{\delta_f \cos(\beta/2)\cos\theta_\tau}. \tag{32}$$

C. Resolution Cell Area

As discussed above, in BSAR the directions of range and azimuth resolutions are not necessarily mutually normal, therefore the resolution cell cannot be sufficiently described only by δ_r and δ_a. For further resolution characterization, it is useful to evaluate the resolution cell area. The area of the resolution cell on the basic plane centered at $\mathbf{A}$ can be expressed by the following integral:

$$S_b = \int_{-\infty}^{\infty}\int_{-\infty}^{\infty}\int_{-\infty}^{\infty} u\left[|\chi(\mathbf{A},[x,y,z]^{\mathrm{T}})| - \frac{1}{\sqrt{2}}\right]\delta \times [([x,y,z]^{\mathrm{T}} - \mathbf{A})^{\mathrm{T}}\mathbf{N}_b]dxdydz \tag{33}$$

where $\mathbf{N_b}$ is the unit vector in the direction of the normal line to the basic plane, $\delta(.)$ is the delta function and $u(.)$ is the step function.

Changing the variables from one coordinate system x,y,z to another x',y',z', where

$$\begin{bmatrix} x' \\ y' \\ z' \end{bmatrix} = \left[\frac{2}{c}\cos\left(\frac{\beta}{2}\right)\boldsymbol{\Theta}, \frac{2\omega_{\mathrm{E}}\boldsymbol{\Xi}}{\lambda}, \mathbf{N}_b\right]^{\mathrm{T}} \left(\begin{bmatrix} x \\ y \\ z \end{bmatrix} - \mathbf{A} \right) \tag{34}$$

(33) takes the form,

$$S_b = \int_{-\infty}^{\infty}\int_{-\infty}^{\infty}\int_{-\infty}^{\infty} u\left[|p(x')m_A(y')| - \frac{1}{\sqrt{2}}\right]\delta(z')|J|dx'dy'dz' = |J|\int_{-\infty}^{\infty}\int_{-\infty}^{\infty} u\left[|p(x')m_A(y')| - \frac{1}{\sqrt{2}}\right]dx'dy'. \tag{35}$$

The Jacobian determinant $|J|$ is

$$|J| = \frac{1}{\left|\left[\frac{2}{c}\cos\left(\frac{\beta}{2}\right)\boldsymbol{\Theta}, \frac{2\omega_{\mathrm{E}}\boldsymbol{\Xi}}{\lambda}, \mathbf{N}_b\right]\right|} = \frac{1}{|[\boldsymbol{\Theta},\mathbf{H},\mathbf{N}_b]|\left|\begin{bmatrix} \frac{2}{c}\cos\left(\frac{\beta}{2}\right) & \cos\alpha\frac{2\omega_{\mathrm{E}}}{\lambda} & 0 \\ 0 & \sin\alpha\frac{2\omega_{\mathrm{E}}}{\lambda} & 0 \\ 0 & 0 & 1 \end{bmatrix}\right|} \tag{36}$$

where $\mathbf{H}$ is a unit vector which perpendicular to both vectors $\boldsymbol{\Theta}$ and $\mathbf{N_b}$, α is the angle between $\boldsymbol{\Theta}$ and $\boldsymbol{\Xi}$. Clearly, $[\boldsymbol{\Theta},\mathbf{H},\mathbf{N}_b]$ is a normalized matrix, therefore $|[\boldsymbol{\Theta},\mathbf{H},\mathbf{N}_b]| = 1$ and as a result we have

$$|J| = \left|\frac{\lambda c}{4\cos(\beta/2)\omega_{\mathrm{E}}\sin\alpha}\right|. \tag{37}$$

After some calculations, (34) can be reduced and the area of a resolution cell can be introduced as

$$S_b = \begin{cases} \dfrac{\pi}{4}\dfrac{\delta_r\delta_a}{\sin\alpha} \\ \quad p(\square) \text{ and } m_A(\square) \text{ are Gaussian functions} \\ 0.794\dfrac{\delta_r\delta_a}{\sin\alpha} \\ \quad p(\square) \text{ and } m_A(\square) \text{ are rectangular shape functions} \end{cases} \tag{38}$$

where again the coefficient in the rectangular model is obtained through numerical integration.

In many applications the resolution cell area on the terrain plane is the most useful. If the angle between the terrain and the basic planes is η, the area of resolution cell on the terrain plane is

$$S_t = \frac{S_b}{\cos\eta}. \tag{39}$$

TABLE II
List of Main Equations

	Expression	Direction
Range resolution	$\delta_r = \dfrac{0.886c}{2\cos(\beta/2)\delta_f}$	$\boldsymbol{\Theta}$
Azimuth resolution	$\delta_a = \dfrac{0.886\lambda}{2\omega_{\mathrm{E}}\delta_u}$	$\boldsymbol{\Xi}$
Cross range resolution	$\delta_c = \dfrac{\delta_a}{\sin\alpha}$	$\mathbf{H}$
Resolution in arbitrary direction	$\delta_{\boldsymbol{\Omega}} = \dfrac{cf(h)}{\delta_f\cos(\beta/2)\cos\theta_\tau}$	$\boldsymbol{\Omega}$
Area of the resolution cell	$S_b = 0.794\dfrac{\delta_r\delta_a}{\sin\alpha}$	
Ambiguity function	$\chi(\mathbf{A},\mathbf{B}) \approx \exp\left(j2\pi\dfrac{[\boldsymbol{\Phi}_{\mathrm{T}A}+\boldsymbol{\Phi}_{\mathrm{R}A}]^{\mathrm{T}}(\mathbf{B}-\mathbf{A})}{\lambda}\right) p\left(\dfrac{2\cos(\beta/2)\boldsymbol{\Theta}^{\mathrm{T}}(\mathbf{B}-\mathbf{A})}{c}\right) m_A\left(\dfrac{2\omega_{\mathrm{E}}\boldsymbol{\Xi}^{\mathrm{T}}(\mathbf{B}-\mathbf{A})}{\lambda}\right)$	

Obviously, the resolution cell on the basic plane possesses the smallest area compared with that on the other planes.

D. Summary

Thus far, a number of useful equations for the BSAR resolution analysis have been derived based on the introduced AF (12) and (24) which describe 1) the resolution in terms of the time delay and Doppler shift, 2) the range resolution, the azimuth resolution, and the resolution in the arbitrary direction, and 3) the area of the resolution cell. To facilitate the usage of the results, the main final equations have been listed in Table II. Having these equations, the resolution in BSAR with a general architecture can be evaluated.

In the remaining part of the paper, we work on the resolution in three kinds of special BSAR geometry. This demonstrates how to analyze the BSAR resolution using the proposed method on the one hand, and clarifies the performance of these systems on the other.

IV. APPLICATIONS

A. Coplanar BSAR Topology

In this subsection, we study a relatively simple (but very important from a practical point of view) BSAR topology, i.e., the coplanar topology where $\mathbf{W}_{\mathrm{T}}$, $\mathbf{W}_{\mathrm{R}}$, $\mathbf{V}_{\mathrm{T}}$, and $\mathbf{V}_{\mathrm{R}}$ are in the same plane. In such a system, the angular difference between the two effective rotation directions is equal to the bistatic angle, therefore the angle between the cross range direction and $\boldsymbol{\Gamma}_{\mathrm{T}}$ (or $\boldsymbol{\Gamma}_{\mathrm{R}}$) is $\beta/2$, and as a result, the cross resolution has quite a simple expression.

Remembering that the azimuth resolution is determined by the combined rotation of the transmitter and receiver while the cross range resolution is the projection of the azimuth resolution on the direction perpendicular to the range direction, let us define M[·] as the projection operator which maps a vector into the cross range direction. This corresponds to the vector's projection length along this direction. Substituting (26) into (27) and using the operator, we find

$$\delta_c = \frac{0.866\lambda}{\delta_u \mathrm{M}[\omega_{\mathrm{T}A}\boldsymbol{\Gamma}_{\mathrm{T}} + \omega_{\mathrm{R}A}\boldsymbol{\Gamma}_{\mathrm{R}}]}. \tag{40}$$

Because the projection operator is linear, we obtain

$$\delta_c = \frac{0.866\lambda}{(\varphi_{\mathrm{T}} + \varphi_{\mathrm{R}})\cos(\beta/2)} \tag{41}$$

where φ_{T} or φ_{R} are the rotation angles of the transmitter or receiver during the time period δ_u. It is seen that (41) specifies the cross range resolution for the given topology and is consistent with the result obtained in [9].

In the coplanar BSAR system, the azimuth and cross range resolutions depend on the bistatic angle as well as the rotation speeds of the transmitter and receiver. Fig. 3 to Fig. 4 show the normalized azimuth and cross range resolution as a function of the bistatic angle, and Fig. 5 shows the angle between $\boldsymbol{\Theta}$ and $\boldsymbol{\Xi}$ as a function of this bistatic angle. In these figures, both the transmitter and receiver rotate clockwise and k indicates the ratio between the angular speed of the receiver and the angular speed of the transmitter. Fig. 6 to Fig. 8 introduce the same dependences in the case where the transmitter and receiver rotate in the opposite direction, i.e., one is clockwise and the other is anticlockwise. For better visualization, a monostatic SAR is imagined to be mounted on the transmitter platform and the bistatic resolutions have been normalized by their monostatic counterparts. Several observations have thus been achieved from these numerical results.

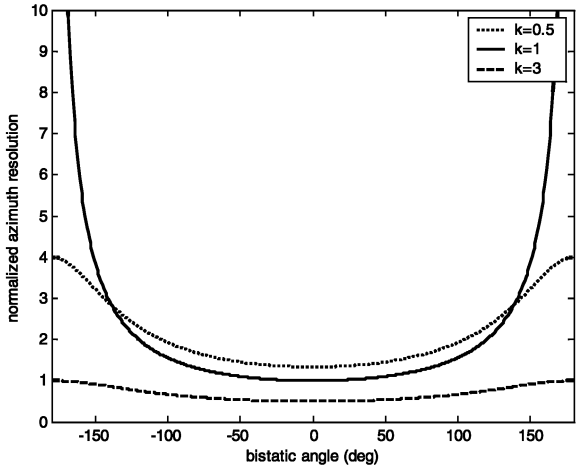

Fig. 3. Normalized azimuth resolution (transmitter and receiver rotate in same direction).

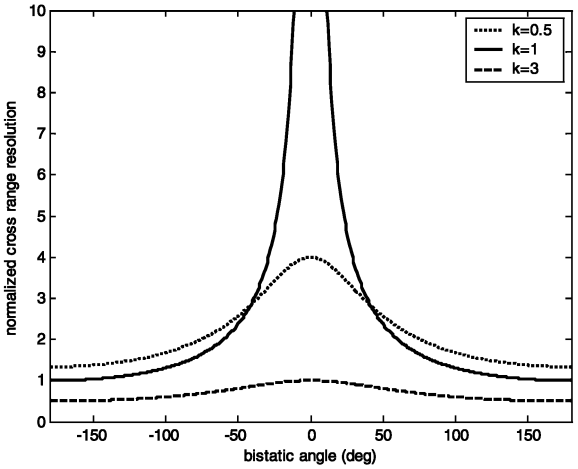

Fig. 6. Normalized azimuth resolution (transmitter and receiver rotate in opposite direction).

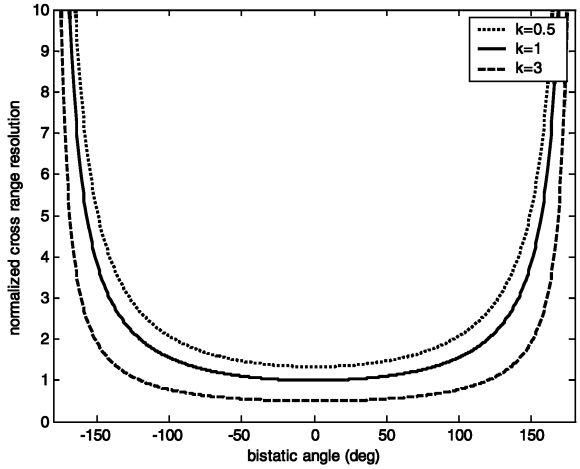

Fig. 4. Normalized cross range resolution (transmitter and receiver rotate in same direction).

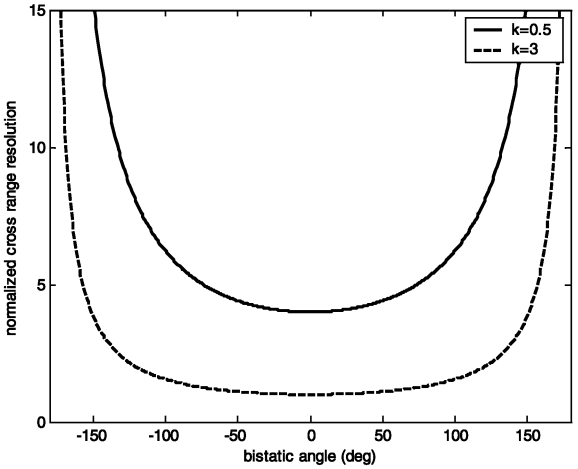

Fig. 7. Normalized cross range resolution (transmitter and receiver rotate in opposite direction).

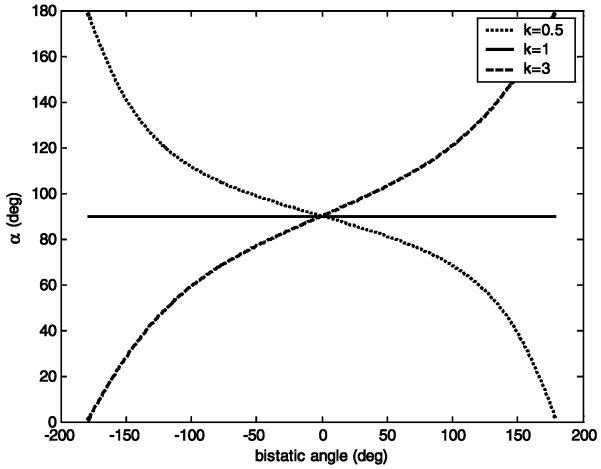

Fig. 5. Angle between azimuth and range directions (transmitter and receiver rotate in same direction).

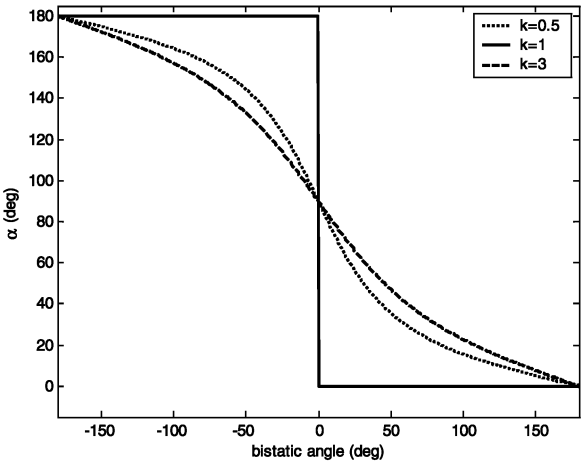

Fig. 8. Angle between azimuth and range directions (transmitter and receiver rotate in opposite direction).

1) Fig. 3 shows that the azimuth resolution decreases when the bistatic angle increases and the degradation speed is very high if the angular speed of the receiver is close to that of the transmitter. Taken to the extremes, i.e., 180 deg bistatic angle, the azimuth resolution will be completely lost if the receiver's angular speed equals the transmitter's ($k = 1$). Fig. 6 also indicates the same trend, but the

worst resolution corresponds to zero bistatic angles. This is due to the fact that the effect of the receiver rotation is compensated by the transmitter's rotation. The comparison of Fig. 3 and Fig. 6 helps to understand the difference between these two BSAR topologies.

2) The direction of the azimuth resolution always coincides with the range resolution's direction if the receiver and the transmitter have equal but opposite directions (see Fig. 8). In this situation, the cross range resolution is totally lost. This topology cannot be used for the two-dimensional BSAR imaging. On the other hand, as reported in [24], it can be useful for a side look moving target indicator (MTI) operation due to fact that the scatter spectrum in each range resolution bin is very narrow.

3) From Fig. 4 and Fig. 7, we know that the value of the cross range resolution will approach infinite when the bistatic angle equals 180 deg. This is due to the fact that the azimuth resolution direction tends to coincide with the direction of the range resolution.

B. Spaceborne BSAR Example

In this subsection, we use equations from Table II to analyze the performance of a spaceborne BSAR system proposed by A. Moccia [23]. Let us recall that the system consists of two satellites. The master satellite possesses a monostatic antenna, i.e., transmitting-receiving antenna. The slave satellite has a receiving-only antenna. Depending on orbit configuration, two mission profiles could be envisaged: the squint mode and the parallel mode. In the squint mode, the two satellites are moving along the same orbit with an appropriate angular separation. In the parallel mode, the two spacecrafts fly along parallel orbits with different ascending nodes, as shown in Fig. 9. In this figure **T** is the monostatic antenna, **R** is the bistatic antenna, **P** is the observed target, **B** is the baseline vector, **W** is the antenna-target slant range, θ is the off-nadir angle, **W** and v are the position and velocity vectors, respectively. The ENVISAT1 can be selected as the master mission, whose main parameters are listed in Table III. To obtain detailed information of the system see [23]. Let us now analyze the resolution ability of this system via the general methods presented in the previous sections of this work. Using the equations in Table II, the ground range and azimuth resolutions are obtained in respect to different baseline length, as shown in Fig. 10 and Fig. 11. The results here have been normalized by the corresponding monostatic resolutions to facilitate visualization. Via these numeric results, we find that the resolution variation is more dynamic in the parallel mode than the squint case. Although a little unexpected, the bistatic resolution could be better than its monostatic counterpart in some cases. For the ground range resolution, this is due

TABLE III
Parameters of ENVISAT1

Orbit	Sunsynchronous
Altitude	800 km
Inclination	98.5 deg
Period	101 minutes
Repeat cycle	35 days

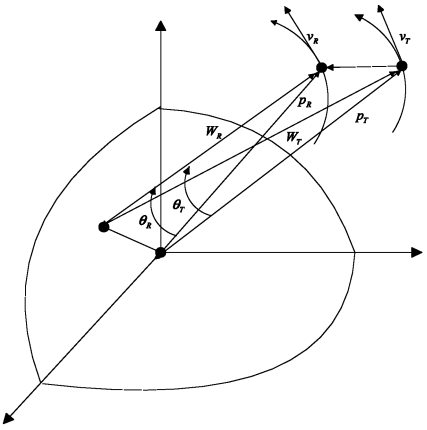

Fig. 9. Orbit configuration of two satellites moving along "parallel orbits."

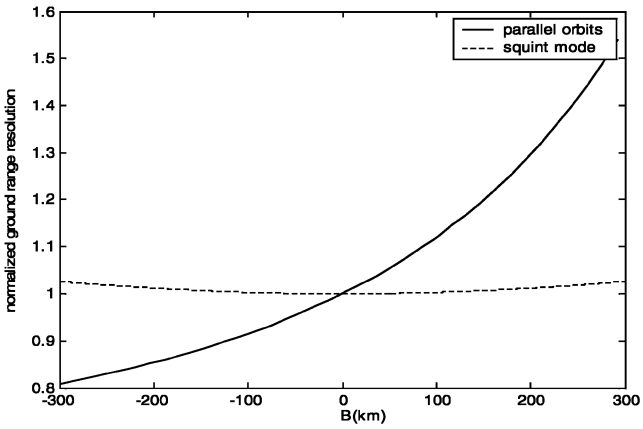

Fig. 10. Ratio between bistatic and monostatic ground range resolutions as function of baseline.

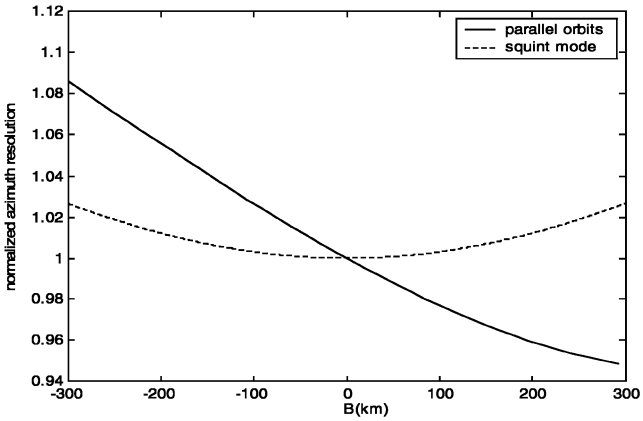

Fig. 11. Ratio between bistatic and monostatic azimuth resolutions as function of baseline.

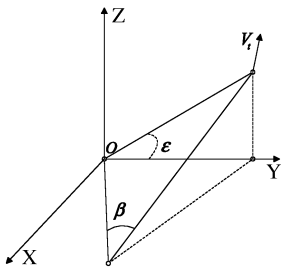

Fig. 12. SS-BSAR coordinate system.

to the fact that the effective grazing angle is smaller than the monostatic SAR if the bistatic receiver is on the outside of the transmitter in the parallel mode. Regarding the azimuth resolution, the bistatic resolution is better when the receiver is on the inside of the transmitter because the angular speed is bigger in such a situation. Results presented in Fig. 10 and Fig. 11 are consistent with those presented in [23] (see Fig. 2 and Fig. 3).

C. SS-BSAR Resolution

Now we demonstrate how to use these general results for the newly introduced system: SS-BSAR resolution study. A comprehensive study of SS-BSAR resolution is beyond the scope of this paper. Surface-space BSAR is described as a SAR with a spaceborne transmitter moving relative to the surface and stationary ground-based receiver [4]. In the SS-BSAR system, it is convenient to establish the coordinate system in such a way that the receiver is at the coordinate origin and the x-O-y plane coincides with the ground plane. As shown in Fig. 12, the nadir of the satellite is on the Y axis and ε is the grazing angle.

The expression of SS-SARs range resolution is just like the general equation but the azimuth resolution is somehow simpler:

$$\begin{aligned} \delta_r &= \frac{c\delta_\tau}{2\cos(\beta/2)} \\ \delta_a &= \frac{\lambda\delta_D}{\omega_{\mathrm{TA}}}. \end{aligned} \tag{42}$$

The most significant parameters of SS-BSAR are δ_x, which is the resolution in the x direction, and δ_y, which is the resolution in the y direction. Let's consider only the Gaussian model. Denoting the angle between $\mathbf{\Gamma}$ and x-axis as θ_{ax}, the angle between $\mathbf{\Theta}$ and x-axis as θ_{rx}, the angle between $\mathbf{\Theta}$ and y-axis as θ_{ay} and the angle between $\mathbf{\Theta}$ and y-axis as θ_{ry}, from (29) the resolutions are

$$\delta_x = \frac{1}{\sqrt{\dfrac{4\cos^2(\beta/2)\cos^2\theta_{rx}}{(c\delta_\tau)^2} + \dfrac{\omega_{\mathrm{TA}}^2\cos^2\theta_{ax}}{(\lambda\delta_D)^2}}} \tag{43}$$

TABLE IV
Simulation Parameters

Satellite altitude	20381 km
Satellite speed	3870 m/s
Satellite motion direction	Parallel with the x axis
Wavelength	0.2 m
δ_τ	33 ns
δ_D	1/200 Hz
Grazing angle ε	30 deg
Under satellite point position	Parameter

and

$$\delta_y = \frac{1}{\sqrt{\dfrac{4\cos^2(\beta/2)\cos^2\theta_{ry}}{(c\delta_\tau)^2} + \dfrac{\omega_{\mathrm{TA}}^2\cos^2\theta_{ay}}{(\lambda\delta_D)^2}}}. \tag{44}$$

In SS-BSAR, the ground plane resolution cell area is

$$S_g = \frac{c\lambda\delta_\tau\delta_D\pi}{8\sin\alpha\cos\eta_g\cos(\beta/2)\omega_{\mathrm{TA}}} \tag{45}$$

where η_g is the angle between the ground plane and the basic planes.

SS-BSAR is a space-variant system, i.e., the resolutions varying with respect to the target's coordinate position. To give a quantitative insight of the performance of SS-BSAR, a simulation was done. The parameters for the simulation are listed in Table IV. Fig. 13 to Fig. 17 show the results, including the spatial variant property of δ_r, δ_a, δ_x, δ_y, and S_g. Two simplified hypotheses have been used in the simulation.

1) The curvature of the Earth has been ignored due to the relatively small observation area of SS-BSAR.

2) The simulation does not include the impact of the Earth rotation. The maximum velocity raised by the rotation is 460 m/s which is relatively small compared with the near 4000 m/s velocity of satellite.

The range resolution is specified by the bistatic angle. The target at the negative half Y-axis has the smallest bistatic angle which equals the grazing angle ε. The bistatic angle for the target at the positive half Y-axis is $180-\varepsilon$ deg which is the biggest in the SS-BSAR topology. Therefore, the lower half plane of Fig. 13 possesses a better resolution than the upper half plane. But the range resolution will not be completely lost, except if the grazing angle is equal 0 deg.

Fig. 14 indicates that the SS-BSARs azimuth resolution is spatial invariant. This is easy predicted and follows from the fact that the azimuth resolution is completely determined by the motion of the satellite in the SS-BSAR system. Although the variation of the target's position will change the slant range slightly, and consequently change the satellite's angular speed, this change is very small due to the high altitude of

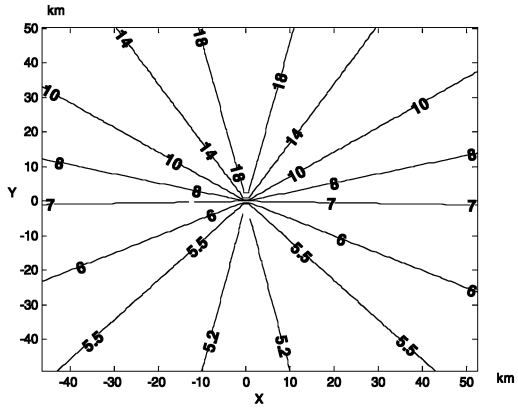

Fig. 13. Range resolution (δ_r).

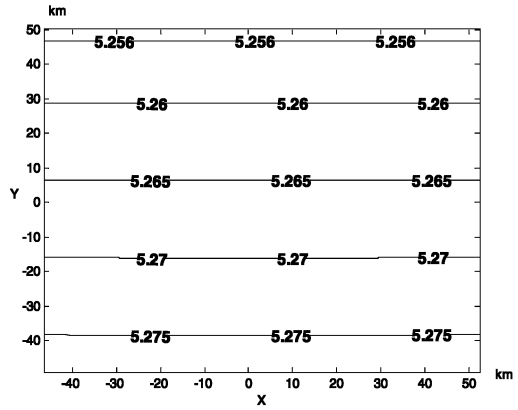

Fig. 14. Azimuth resolution (δ_a).

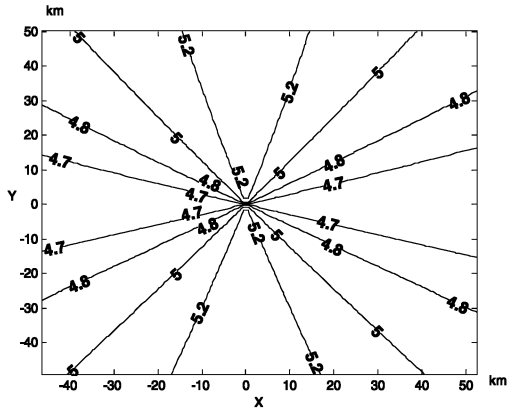

Fig. 15. Resolution in X direction (δ_x).

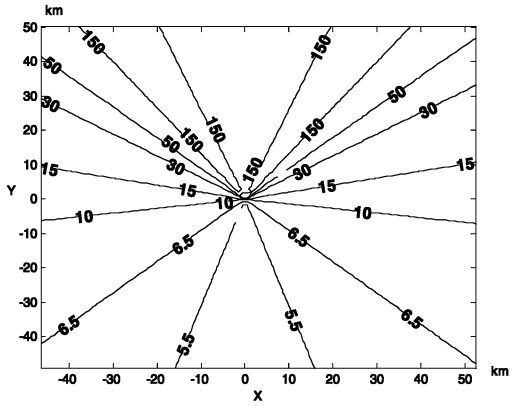

Fig. 16. Resolution in Y direction (δ_y).

the satellite and can be ignored from an engineering point of view.

According to the geometry shown in Fig. 12, δ_x is determined mainly by the azimuth resolution and δ_y determined by the range resolution. As a result, the variation of δ_y is much more dramatic than the variation of δ_x, as shown in Fig. 15 and Fig. 16. We also notice in Fig. 16 that δ_y is much larger than the range resolution when the target is near the positive half Y axis; this is due to the angle between Y axis and that the direction of the range resolution is quite sizeable in this region.

V. CONCLUSION

In this paper, the GAF of bistatic SAR is introduced. Through the study of the amplitude of the AF, the equations of the resolution of BSAR are presented. Here, we also point out that the phase of AF plays a key role in the interferometry. In future work, the performance of the interferometric bistatic SAR will be studied by the usage of the phase of the GAF.

Using this basic approach, two sets of equations are deduced to characterize resolution in terms of delay-Doppler and space coordinates. The resolution was specified as range and azimuth resolutions, as well as the resolution cell area. Moreover, it was derived from appropriate equations that specify resolution in basic and arbitrary planes. The proposed method can be viewed as a universal and powerful tool for BSAR systems analysis. On the other hand, by using SS-BSAR as a test case, it was demonstrated how resolution analysis of any particular BSAR configuration can easily be done. The correctness of the proposed generalized method is verified by the results in comparison to particular configurations obtained by other approaches to the resolution study.

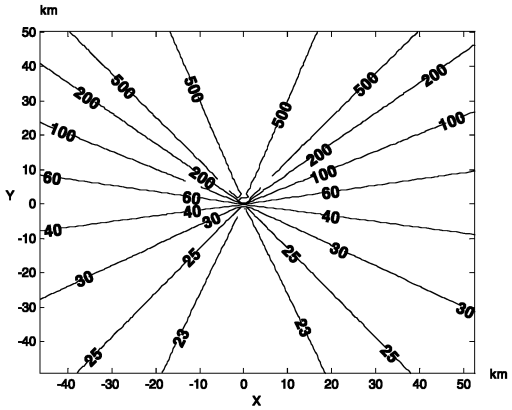

Fig. 17. Ground resolution area (S_g).

REFERENCES

[1] Moccia, A., Rufino, G., D'Errico, M., Alberti, G., et. al.
BISSAT: A bistatic SAR for Earth observation.
In *Proceedings of IEEE International Geoscience and Remote Sensing Symposium* (IGARSS'02), *Vol. 5*, June 24–28, 2002, 2628–2630.

[2] Zavorotny, V. U., and Voronovich, A. G.
Scattering of GPS signals from the ocean with wind remote sensing application.
IEEE Transactions on Geoscience and Remote Sensing, **38**, 2 (Mar. 2000), 951–964.

[3] Cherniakov, M., Zeng T., and Plakidis, E.
GALILEO signal based bistatic system for avalanche prediction.
Presented at the International Conference of Geoscience and Remote Sensing (IGARSS-03), Toulouse, France, 2003.

[4] Cherniakov, M.
Space-surface bistatic synthetic aperture radar—Prospective and problems.
Presented at the International Conference of Radar-2002, Edinburgh, UK, 2002, 22–26.

[5] D'Errico, M., and Moccia, A.
The BISSAT mission: A bistatic SAR operating in formation with COSMO/SkyMed X-band radar.
In *IEEE Aerospace Conference Proceedings, Vol. 2*, Mar. 9–16, 2002, 2-809–2-818.

[6] Woodward, P. M.
Probability and Information Theory, with Applications to Radar.
Norwood, MA: Artech House, 1980.

[7] Skolnik, M.
Radar Handbook.
New York: McGraw-Hill, 1990, sect. 21.4.

[8] Soumekh, M.
Synthetic Aperture Radar Signal Processing.
New York: Wiley, 1999.

[9] Willis, N.
Bistatic Radar.
Norwood, MA: Artech House, 1991.

[10] Whitewood A., Muller B., Griffiths H., and Baker, C.
Bistatic SAR with application to moving target detection.
Presented at the International Conference RADAR-2003, Adelaide, Australia, 2003.

[11] Guttrich, G. L., and Sievers, W. E.
Wide area surveillance concepts based on geosynchronous illumination and bistatic UAV or satellite reception.
In *IEEE Aerospace Conference Proceedings*, Aspen, CO, 1997, 171–180.

[12] Cardillo, G. P.
On the use of the gradient to determine bistatic SAR resolution.
In *Proceedings of AP-S International Symposium, Vol. 2*, 1990, 1032–1035.

[13] Van Trees, H. L.
Detection, Estimation, and Modulation Theory.
New York: Wiley, 1971.

[14] Oppenheim, A. V., Willsky, A. S., and Young, I. T.
Signal and System.
Englewood Cliffs, NJ: Prentice-Hall, 1983.

[15] Rosen P. A., Hensley, S., Joughin, I. R., Li, F. K., Madsen, S. N., Rodriguez, E., and Goldstein, R. M.
Synthetic aperture radar interferometry.
Proceedings of the IEEE, **88**, 3 (2000), 333–382.

[16] Currie, A., Baker, C. J., Bullock, R., Edwards, R., and Griffiths, H. D.
High resolution 3-D radar imaging.
In *IEEE National Radar Conference Proceedings*, 1995, 468–472.

[17] Cherniakov M., Kubik, K., and Nezlin, D.
Bistatic synthetic aperture radar with non-cooperative LEOS based transmitter.
In *Proceedings of International Conference on Geoscience and Remote Sensing Symposium* (IGARSS-2000), 2000, 834–837.

[18] Cherniakov, M., Kubik, K., and Nezlin, D.
Radar sensors based on communication LEOS microwave emission.
In *Proceedings of International Conference on Geoscience and Remote Sensing Symposium* (IGARSS-2000), Hawaii, 2000, 1007–1008.

[19] Cherniakov, M., and Kubik, K.
Secondary applications of wireless technology.
In *Proceedings of the International Conference on ECWT-2000*, France, 2000, 305–309.

[20] Cherniakov, M., Zeng, T., and Plakidis, E.
Ambiguity function for bistatic SAR and its application in SS-BSAR performance analysis.
Presented at the International Conference RADAR—2003, Adelaide, Australia, 2003.

[21] Tsao, T., Slamani, M., Varshney, P., Weiner, D., and Schwarzlander, H.
Ambiguity function for a bistatic radar.
IEEE Transactions on Aerospace and Electronic Systems, **33**, 3 (1997), 1041–1051.

[22] Moyer, L. R., Morgan, C. J., and Rugger, D. A.
An exact expression for resolution cell area in special case of bistatic radar systems.
IEEE Transactions on Aerospace and Electronic Systems, **25**, 4 (1989), 584–587.

[23] Moccia, A., Chiacchio, N., and Capone, A.
Spaceborne bistatic synthetic aperture radar for remote sensing applications.
International Journal of Remote Sensing, **21**, 18 (2000), 3395–3414.

[24] Gaspare, G.
Advanced Radar Techniques and Systems, New York: Peregrinus, Ltd., 1993.

Tao Zeng received his Ph.D. degree in 1999 from the Department of Electronic Engineering, Beijing Institute of Technology, China.

He joined the teaching staff of the same university in 1999. His research interests include SAR imaging technology and real time radar signal processing.

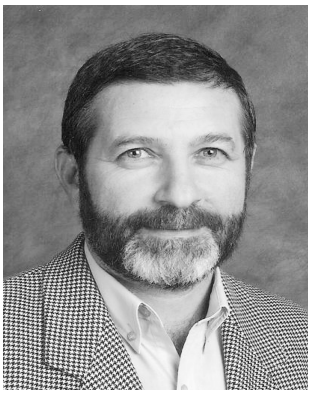

Mikhail Cherniakov received the M.Eng. (1974), Ph.D. (1980), and D.Sc. (1992) in the Technical University, Moscow Institute of Electronics Engineering (Russia, MIEE).

After 1974 he was with the Department of Microwave Systems at MIEE. In 1981 he became the founding head of the Microwave Systems R&D Laboratory. In 1992 he accepted an appointment as professor in MIEE. In 1994 he was a visiting professor in Cambridge University, UK. From 1995 he was with the Department of Information Technology and Electrical Engineering, University of Queensland, Australia. He joined the Communications Engineering Group at the University of Birmingham, UK, in April 2000. The area of his research activity is system aspect of radar and mobile communications and in particular ultra-wideband radar, multisite and forward scattering sensoring, and systems with active phased array as well as selected problems of digital signal processing.

Dr. Cherniakov is the author of more than 100 papers, 10 patents, and one monograph.

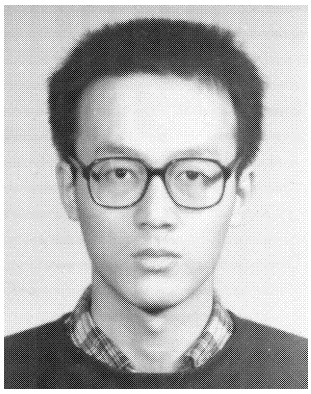

Teng Long was born in 1968, in the Province of Fujing, P.R. China. He graduated with a degree in radio electronics from the University of Science and Technology of China in 1989. He received his Ph.D. electronic engineering from the Beijing Institute of Technology (BIT) in 1995.

He became a lecturer in the Electronic Engineering Department of BIT and now is a full professor there. From January to August of 1999, he was a visiting associate professor at Stanford University, Stanford, CA. From March to September of 2002, he was a visiting scholar at the University College of London. His research is mainly about digital signal processing, with applications to radar and communication systems.